NOLTA, IEICE

Invited Paper

Risk management in spatio-temporally varying field by true slime mold

Kentaro Ito [1 a)], *David Sumpter* [2], *and Toshiyuki Nakagaki* [3,4]

[1] *Department of Mathematical and Life Sciences, Hiroshima University, Kagamiyama 1-3-1, Higashi-Hiroshima, 739-8526, Japan*

[2] *Mathematics Department, Uppsala University, SE-751 05 Uppsala, Sweden*

[3] *Department of Complex and Intelligent Systems, Faculty of Systems Information Science, Future University Hakodate, Kamedanakano 116-2, Hakodate, 041-8655, Japan*

[4] *JST, CREST, 5, Sanbancho, Chiyoda-ku, Tokyo, 102-0075, Japan*

[a)] *kentaro@hiroshima-u.ac.jp*

Abstract: Revealing how lower organisms solve complicated problems is a challenging research area, which could reveal the evolutionary origin of biological information processing. Here we report on the ability of a single-celled organism, true slime mold, to find a smart solution of risk management under spatio-temporally varying conditions. We designed test conditions under which there were three food-locations at vertices of equilateral triangle and a toxic light illuminated the organism on alternating halves of the triangle. We found that the organism behavior depended on the period of the repeated illumination, even though the total exposure time was kept the same . A simple mathematical model for the experimental results is proposed from a dynamical system point of view. We discuss our results in the context of a strategy of risk management by *Physarum*.

Key Words: *Physarum*, bio-computing, ethology, amoeba, dynamic optimization, nonlinear dynamics

1. Introduction

Many organisms living in their natural environments are exposed to not only spatial but also to temporal variations of their surroundings. Thus, even for single-celled organisms, it is reasonable to expect that an ability to adapt to such external variations is necessary. *Physarum* has become a model organism for study of problem solving by single organisms. In the last decade, it has been shown that the organism can find the optimum solution in some geometrical puzzles: maze, shortest network problem, risk-minimum path problem and multi-objective optimization problem [1–10]. In these experiments, however, the experimental conditions are temporally constant while being spatially inhomogeneous.

Little is currently known about these and other simple organisms ability to deal with a combination

[Received: June 29, 2010. Published: October 1, 2010.]
[DOI: 10.1588/nolta.1.26]
Nonlinear Theory and Its Applications, IEICE, vol. 1, no. 1, pp. 26−36

of spatial and temporal variations. What is known is that *Physarum polycephalum* can show anticipatory behaviors in response to a temporally periodic stimulations of environmental conditions while the spatial conditions are homogeneous [11]. This means that *Physarum* can adapt to the dynamic environments. Combining the spatial and the temporal variations is reasonable next step in further investigation of biological information processing by single cell organisms.

The basic biology of *Physarum* is reviewed in [12, 13]. Its body consists of a network of veins which rearranges when migrating. This network plays a key role for transport of body mass and for circulation of nutrients and signals through the body. The shape of the network changes in response to variations of external conditions. For instance, *Physarum* traces the shortest connection path through a thick tube between two distant food sources [1]. For the case of three food sources placed at the vertices of equilateral triangle, the tube network connects all of three food sources through various kinds of network shape [5, 7]. The network of minimum total length named "Steiner Tree" being one of the potential solutions. *Physarum* can find a smart network solution under the spatially inhomogeneous fields [14, 15].

In this report, we study the computational ability of *Physarum polycephalum* when confronted with a problem with both spatio-temporally varying conditions. Here we consider an experimental setup which is as simple as possible. We place three food sources on the vertices of equilateral triangle. To involve the temporal variations, we apply light illumination to a half part of the triangle, and alternately switch illumination from one half to the other. This light is toxic and induces the organism to avoid it [4]. Under such conditions, the plasmodium should gather at the food sources in order to absorb nutrients but, on the other hand, it should also aim to maintain a large body as a whole. In general, this organism is not likely to separate into subsystems. Understanding the strategy for trade-off between gathering food and the maintaining unity is not trivial. What we want to know here is what the organism's strategy is when faced with a dynamic problem and how it solves this problem.

Since behaviors of organism are output from information processing, we may collect a hint at the information processing perfomed by the organism. In *Physarum*, the behavior is reflected by the visible shape of tube network. In understanding the mechanisms of *Physarum* we are helped by a well-established mathematical model for ethological dynamics that has already been proposed for either spatial variations [15, 16] or temporal variations [11]. Based on the model, we proposed a possible mechanism analyzed by means of dynamical systems theory.

2. Experimental study

2.1 Materials and methods

The plasmodium of *Physarum polycepharum*, which regenerated from the sclerotia and starved for 12 hr in the dark, were served for the experiment. A plastic film was placed onto a 1 % agar gel, leaving

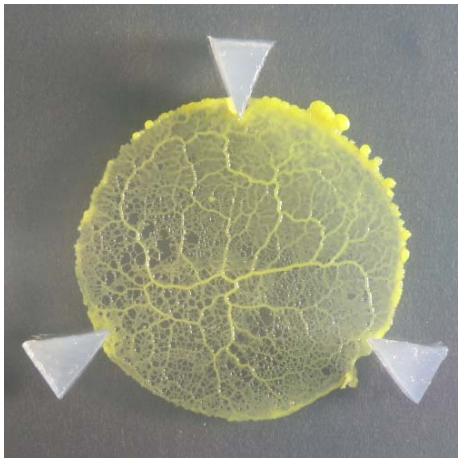

Fig. 1. Network shape just after the presentation of three FSs. The diameter of circle was 3 cm.

a circular area (diameter = 3 cm) of the gel uncovered. A frontal piece (40 mg) of the plasmodium was cut from a large plasmodium (20×30 cm^2) and placed in the circular open area. This preparation was placed in the dark for a few hours until the plasmodium spread entirely over the open area. The plastic film was removed carefully, ensuring that the specimen was not damaged. Three equal-sized agar blocks (1% agar in water), which contained glucose (1.8 mg/ml) and Casamino acid (2.0 mg/ml), were then presented at the vertices of an equilateral triangle as shown in Fig. 1. The agar block was food source or FS in short hereafter.

In order to introduce spatio-temporal variations, soon after the presentation of food blocks we illuminated the toxic light on each half of the specimen in turn for a period of $P = 30, 60$ and 90 min. Therefore, each half was illuminated for a period of time P and then kept in the dark for a period of time P, and the cycle was repeated. So one cycle of illumination took a period of time $2P$. Figure 2 illustrates this process, showing the patterns of illumination for each half of the sample, which were switched from one half to the other after each time period P. White region in Fig. 2 corresponds illuminated field. The light pattern was produced using a laptop computer and projected onto the sample from the projector (type NP2150, NEC (Nippon Electric Company), Tokyo, Japan). The light was reflected from the mirror surface placed above the specimen. The strength of illumination is 21000 lx. The strong illumination gives rise to the intracellular production of reactive oxygen species which are avoided by the organism. At the beginning of the illumination, the right half was illuminated before the left half.

Six hours after the illumination, the resulting network shapes were observed. Network shape that connected the FSs was characterized by topology of connectivity through relatively thick tubes only as many thin tubes were neglected. The point to characterize the network shape was which FSs were connected each other through thick tubes.

2.2 Results

After we started the illumination in any periods of switching, the organism moved toward the FSs, and tubes gradually grew thick or diminished. Figure 3 shows several examples of the network shape arising in the experiment. The shape arising depended on the period of switching illumination. For $P = 30$ min., all of three FSs remained connected through a few thick tubes, as shown in Figs. 3a and b. For $P = 60$ min., the pattern sometimes lacked a direct connection between the top FS and the right bottom FS (Fig. 3c) although it was also sometimes observed that three FSs were connected similarly to that in $P = 30$ min. For $P = 90$ min., the network that connected all of three FSs was no longer observed (Fig. 3d and e). The network shapes showed two types: the two bottoms of FS were connected but the top FS was isolated (Fig. 3d), and all of three were isolated (Fig. 3e).

The final patterns can be better understood by considering the dynamics in the 60 minute case. Figure 4 shows a time course of network shape for $P = 60$ min. Just after the light illumination, the

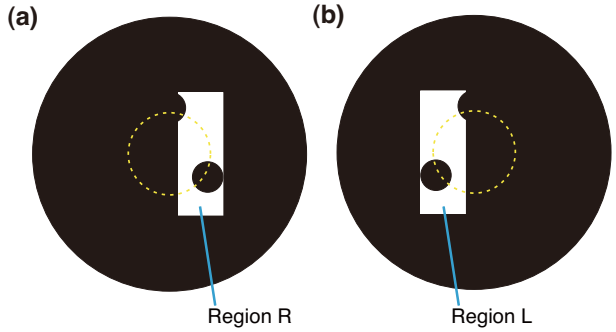

Fig. 2. Illumination patterns on the slime mold. White part corresponds illuminated region. (a) region R: illumination on right hand side, (b) region L: illumination on right hand side. Light intensity of white area is about 21000 lx. Region R was illuminated first, and region R and L were switched in a constant period P (The entire cycle of alternate illumination was $2P$). Dotted circle corresponds initial boundary of slime mold.

available circular space was filled with the plasmodium (Fig. 4a). The organism gathered at all FSs and left some tubes to maintain connections among the FSs one hour after the illumination (Fig. 4b). Finally there existed only two thick tubes that connected the top FS to the left bottom FS, and the left bottom FS and to the right bottom FS.

Figure 5 shows statistics of final network patterns under each condition (P = 30 min, 60 min, 90 min), which were classified into four groups by focusing on relatively thick tubes only. In the first group in Fig. 5, the network connected all three FSs, and the density of network edges was similar in the two right and left halves. In the second group, the network connected all of three FSs but the FSs 1 and 3 were not directly connected in region R. Importantly, region R is the half which was illuminated first and then lacked a direct connection. In general, density of network edges was always lower in region R. Thus for these shapes the left-right symmetry was lost in the network shape. In the third group in Fig. 5, the network connected two FSs 2 and 3 only. The FS 1 was isolated. No clear difference of edge density was observed between the two halves. As a result the left-right symmetry

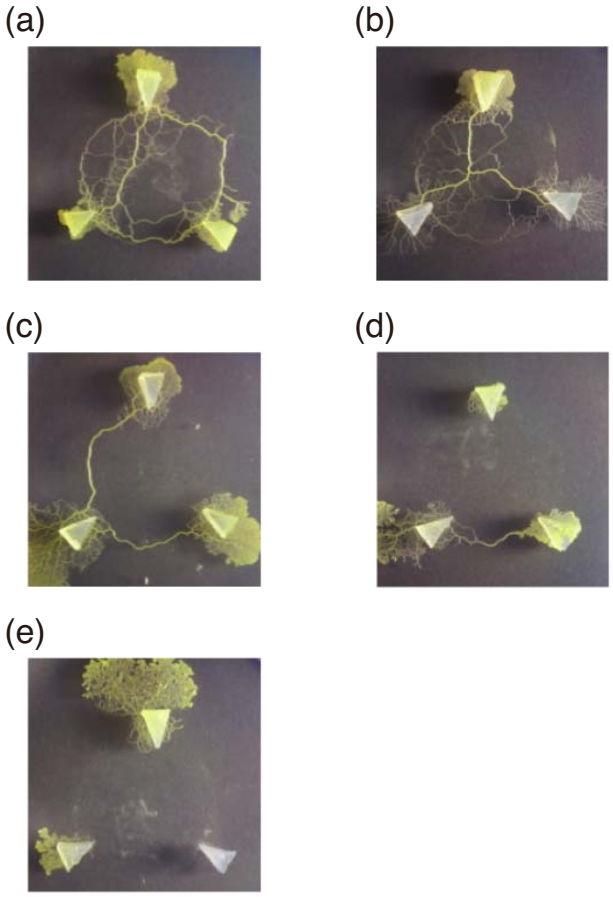

Fig. 3. Several final pattern of network. The network pattern is illustrated 6 hours after FS presentation. Illuminated region was changed every (a)(b) 30 min, (c) 60 min, (d)(e) 90 min.

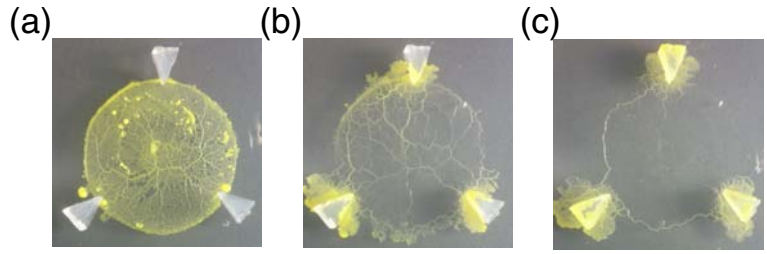

Fig. 4. Time course of network shape in $P = 60$ min. (a) 0 hour, (b) 1 hour, (c) 2 hours after starting the light illumination.

was recovered. The forth group was the network shape that did not connect any FSs. All of three FSs were isolated.

As described above, total length of thick-tube network tended to get shorter as P increased although total exposure time of light illumination was the same in every P. Another nontrivial result was that left-right symmetry was lost only in $P = 60$ min., while it was held for the other periods $P = 30, 90$ min. These results mean that the organism was able to react to combination of spacial and temporal variations of surroundings. In the next section, we consider a mathematical model for the observed behaviors which helps us understand these observations.

3. Mathematical model

Actual processes of cell dynamics of *Physarum* are too complex to treat in a straightforward manner. Here we neglect the complexity of aspects such as viscoelastic characters and biochemical reactions. Let us begin with a simple model for adaptive network of tube in *Physarum*, previously proposed in the references [14–16]. The main concept of this model is that tube network is modeled by network of water pipes, in which thickness of pipe varies in response to flow through the pipe itself. If the flow is large enough, pipe becomes thicker, whereas if flow is small, pipe thins and collapses. We suppose that the initial condition of the network is a regular triangle in which vertices and edges correspond positions of FSs and tubes, respectively. We then run the model to try to reproduce the basic tendency of the final pattern with respect to the period P.

3.1 Standard *Physarum* model

First we briefly introduce background of the already proposed model. Suppose that the pressure at nodes i and j are p_i and p_j, respectively. The variable Q_{ij} denotes the flux through a tube, which is connecting nodes i and j, of length l_{ij} and radius r_{ij} for a cylindrical hard pipe. Assuming that flow is laminar and follows the Hagen-Poiseuille equation, the flux through the tube is then given by

$$Q_{ij} = \frac{D_{ij}(p_i - p_j)}{l_{ij}}. \tag{1}$$

The conductance D_{ij} is translated to tube thickness r_{ij} by the equation, $D_{ij} = \pi r_{ij}^4/8\eta$, where η is viscosity of fluid. The conductivity D_{ij} evolves according to the following equation,

$$\frac{dD_{ij}}{dt} = f(|Q_{ij}|) - c_{ij}D_{ij}. \tag{2}$$

The first term in right-hand side represents adaptive change in tube conductance, which is given by $f(Q_{ij}) = |Q_{ij}|^\gamma/(1 + |Q_{ij}|^\gamma)$, where γ is a model parameter. The second term in right-hand side describes constriction of the tube with decay rate $c_{ij} > 0$. It means that tubes will gradually disappear if Q_{ij} is zero (no flow). That's a summary of the previous model that is a basis for our model. Please see the references for the details [15, 16].

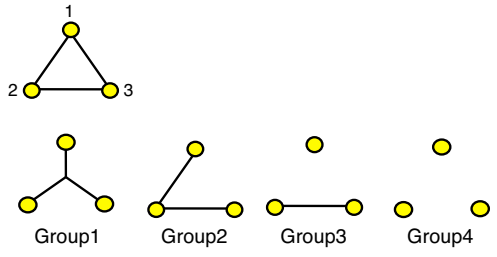

	Group1	Group2	Group3	Group4
P=30min	10	0	0	0
P=60min	7	3	0	0
P=90min	0	0	4	2

Fig. 5. Statistics of network shape 6 hours after starting illumination. Numbers in the table means numbers of specimen that showed the shape. Number of repeats were 10 for $P = 30, 60$ min or 6 for$P = 90$ min. The circles correspond FSs, and the solid edges correspond connection between FSs.

3.2 Model extension for temporal variations

Figure 6 shows a schematic illustration of our model including temporal dynamics. Because of the photophobic nature of this organism, an edge in illuminated region tends to disappear quickly, therefore $c_{ij}(t)$ in illuminated region is larger than that in the dark region. When the edge is partially illuminated, the decay rate $c_{ij}(t)$ should take an intermediate value between the values under entirely illuminated conditions and under dark conditions. $c_{ij}(t)$ is a time-periodic step function with a period $2P$.

According to the conventional consideration in the previous model, $p_i(t)$ is periodic with period T, but the period is much shorter than P. This assumption is still reasonable in our current model, because thickness of the slime mold periodically oscillates in the period of 1 to 2 min., and the switching period of illumination is at shortest 30 min. For simplicity, we assume that $p_1(t) = p_2(t + T/3) = p_3(t + 2T/3)$. Therefore p_i averaged over the time interval $[t, t + T]$ gives an approximation for the original system Eq. (2), and the equations

$$Q_{ij} = \alpha D_{ij}, \tag{3}$$

$$\alpha = \frac{1}{T}\int_{t_0}^{t_0+T} \frac{|p_i - p_j|}{l_{ij}} dt, \tag{4}$$

are holds, where α is constant, although p_i and p_j are time-dependent. The averaging method allows us to ignore the time variation of pressure. This is a point.

For simplicity, we replace D_{12}, D_{13} and D_{23} by D_1, D_2, D_3, respectively. Equation (2) can be rewritten as the following equation,

$$\frac{dD_i}{dt} = F(D_i) - c_i D_i, \tag{5}$$

where $F(D_i) = D_i^\gamma/(\beta + D_i^\gamma)$ and $\beta = \alpha^{-\gamma}$ in general. We assume $\beta = 0.03$, $\gamma = 3.0$ as a typical set of value in this paper. c_1 c_2, and c_3 represent c_{12}, c_{13} and c_{23}, respectively, and can be written as the following,

$$(c_1, c_2, c_3) = \begin{cases} (1, 2, 1.5) & (2nP \le t < (2n+1)P) \\ (2, 1, 1.5) & ((2n+1)P \le t < (2n+2)P), \end{cases} \tag{6}$$

where n is non-negative integer, as shown in Fig. 6. According to the previous papers [4, 15], values of c_i is to be approximately in a range of 1.2 to 2.2 for the light intensity of 20000 to 80000 lx when it is 1 for dark condition. Here we set $c = 1$ for the dark and $c = 2$ for the entire illumination. The model results do not however critically depend on this parameter value. When the edge 1 with c_1 is under illumination for a period P and under dark for the next period P, the edge 2 with c_2 is under dark first for P and under illumination for the next P. Thus the c values 1 and 2 are alternate between c_1 and c_2. For the edge 3, the c_3 value is constant at $c_3 = 1.5$ because just half length of tube is always illuminated: only half length is illuminated for a period P, and another half is illuminated for the next P.

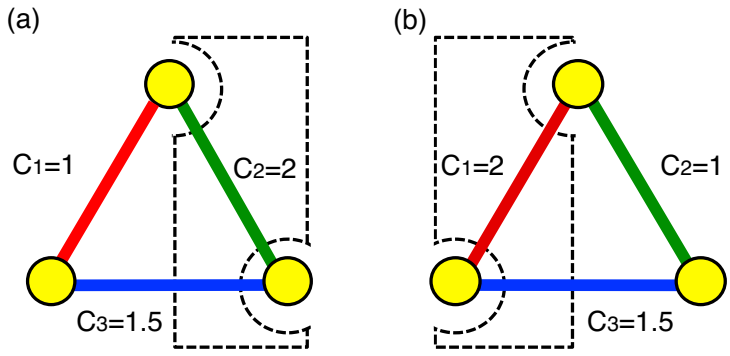

Fig. 6. Decay rate c for each edge. A domain bounded by dashed lines represents illuminated area. (a) $2nP \le t < (2n+1)P$, (b) $(2n+1)P \le t < (2n+2)P$.

3.3 Analysis of the temporally constant conditions

To understand the behavior of Eq. (5), we first consider the following equation,

$$\frac{dD}{dt} = F(D) - cD, \tag{7}$$

where time dependency of environmental variations is to be neglected.

Figure 7 shows time derivative of D for $c = 1, 1.5, 2$. It is clear that $D = 0$ is a stable fixed point for all cases. Equation (7) can have two more fixed points, an unstable fixed point $D_u(c)$ and a stable fixed point $D_s(c)$, at $c = 1$ and 1.5. When these fixed points exist, the asymptotic behavior of $D(t)$ can be described in terms of the initial conditions $D(0)$. $D(t)$ converges to 0 if $D(0) < D_u(c)$, while $D(t)$ converges to $D_s(c)$ if $D(0) > D_u(c)$. The pair of unstable and stable fixed points coalesces and disappears when c exceeds a critical value (called a saddle-node bifurcation). Thus $D = 0$ is the only fixed point at $c = 2$, and it means that $D(t)$ gradually approaches 0 for any initial condition $D(0)$.

3.4 Dynamical behavior for the spatio-temporally variations of external conditions

Based on the above analysis for temporally constant conditions, we now involve the switching of illumination. It is clear that the asymptotic behavior of $D_3(t)$ depends on its initial condition. The dynamics of $D_3(t)$ does not depend on P, because c_3 is constant at 1.5. Thus it shows the same dynamics as $D(t)$ at $c = 1.5$. Dynamics of D_1 and D_2 are more complex. For simplicity we restrict the initial conditions to $D_1(0) = D_2(0) = D_3(0) = D_0 > 0$ after this. For P is sufficiently small, $D_1(t)$ and $D_2(t)$ are in a neighborhood of $D_3(t)$ for $t > 0$. Thus, eventually, $D_1(t)$ and $D_2(t)$ oscillate around $D_s(1.5)$ if $D_0 > D_u(1.5)$, and converge to 0 if $D_0 < D_u(1.5)$.

For sufficiently large P, $D_1(t)$ and $D_2(t)$ converge to 0 for any D_0. This can be explained as follows. For $D_0 > 0$, dD/dt is always negative if c = 2, thus there exists $t_1 < 2P$ and $t_2 < P$, such that $D_1(t_1), D_2(t_2) < D_u(1)$ when P is sufficiently large. As shown in Fig. 7, once $D_1(t)$ and $D_2(t)$ fall below $D_u(1)$, the time derivation $dD_1/dt, dD_2/dt$ never become positive, even when the illumination is switched off. The tube formation has fallen below the unstable threshold and is unable to recover. Thus $D_1(t)$ and $D_2(t)$ converge to 0.

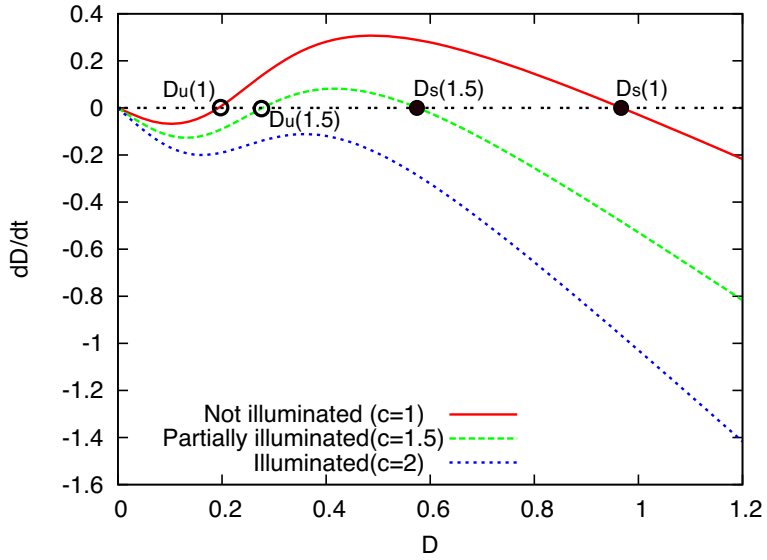

Fig. 7. Time derivative of D in Eq. (7). Solid line represents dD/dt when the edge is in a dark region ($c = 1.0$). Dashed line represents dD/dt when the edge is partially illuminated ($c = 1.5$). Dotted line represents dD/dt in illuminated region ($c = 2.0$). Open circle and black circle represent unstable equilibrium and stable equilibrium, respectively. $D_u(1)$ and $D_s(1)$ are unstable fixed point and stable fixed point at $c = 1$. $D_u(1.5)$ and $D_s(1.5)$ are unstable fixed point and stable fixed point at $c = 1.5$.

While the asymptotic behaviors of $D_i(t)$ at extremely large P and extremely small P can be understood by analysis of the temporally constant condition as Eq. (7) it is less clear what happens if P has an intermediate. Figure 8 shows time series of D_1, D_2, D_3 for several P. As shown the numerical calculation and the result of our experiment. Figure 3 shows same tendency, $D_1(t)$, $D_2(t)$, $D_3(t)$ remains at small P, only $D_2(t)$ goes to 0 at middle P, and $D_1(t)$ and $D_2(t)$ goes 0 at large P. These results are dependent on initial conditions and it is also possible that $D_2(t)$ remains positive for intermediate P, as occurred in some experiments. In general, however the greater the frequency the less paths between the food sources.

3.5 Analysis of discrete dynamical system

To understand the dynamical behavior of Eq. (5) for the intermediate P, we transfer the continuous system into a discrete dynamical system. Because of time periodicity of $c_i(t)$, $D_1((2n+2)P)$ is uniquely determined by $D_1(2nP)$ where n is non-negative integer. Thus, a map $M : D_1(2nP) \mapsto D_1((2n+2)P)$ can be determined. Figure 9 shows the map M, *i.e.*, $D_1((2n+2)P) = M(D_1(2nP))$, at several P. For $P < 2.913$, the map M has a positive unstable fixed point $\bar{D}_u$ and a positive stable fixed point $\bar{D}_s$. At $P = 2.913$, the two fixed points collide into one a neutral stable fixed point $\bar{D}_n$, and no positive fixed points remain for $P > 2.913$, *i.e.*, a saddle-node bifurcation occurs. Note that a positive fixed point of map M does not correspond to an equilibrium of the Eq. (5), and they correspond to periodic orbits in the original system.

Asymptotic behavior of $D_1(t)$ can now be explained. For $P < 2.913$, $D_1(2nP)$ approaches $\bar{D}_s$. Asymptotic behavior of $D_2(t)$ can be also understood by the M, because M represents not only $D_1(2nP) \mapsto D_1((2n+2)P)$ but also $D_2((2n+1)P) \mapsto D_2((2n+3)P)$. Thus if $D_1(0) = D_2(P)$, $D_1(2nP) = D_2((2n+1)P)$ holds at an arbitrary $n \geq 0$. If $D_1(0) = D_2(0)$, $D_1(0) > D_2(P)$ generally, because as shown in Fig. 7, $dD_2(t)/dt < 0$ for $0 < t < P$. The asymptotic behavior of $D_1(t)$, $D_2(t)$

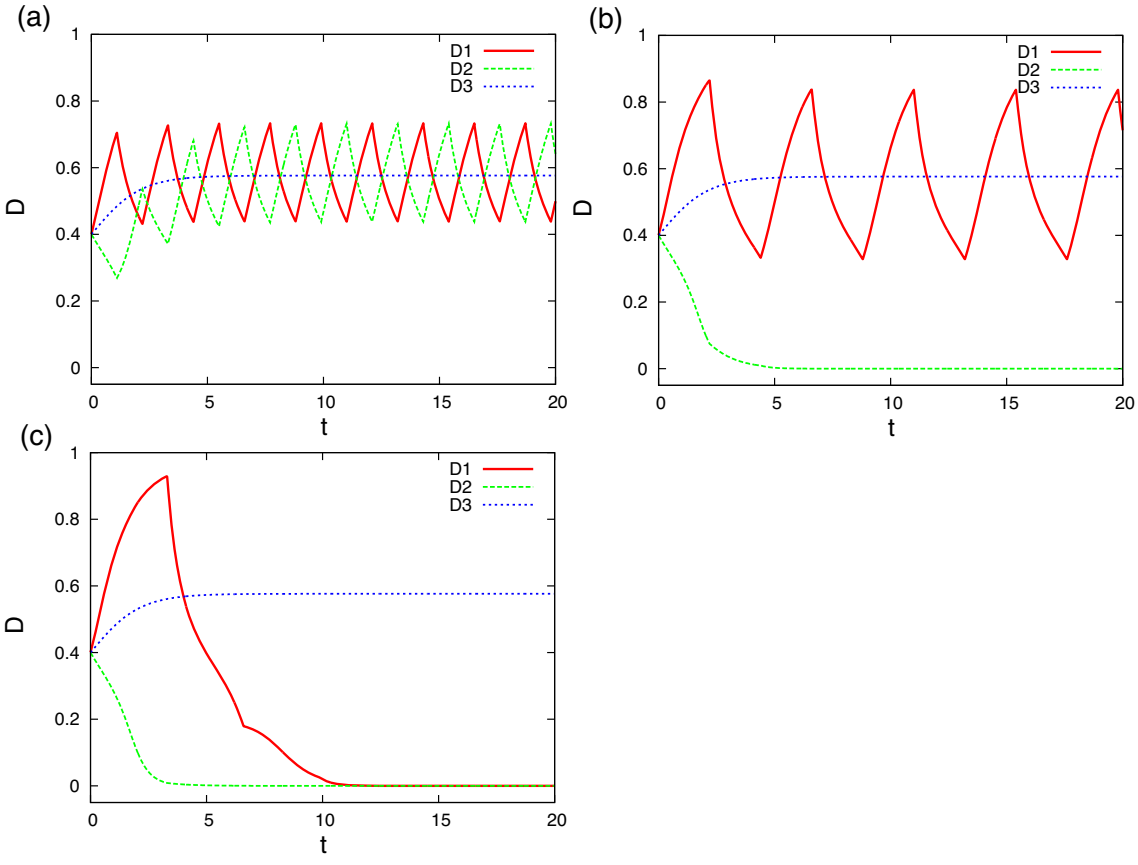

Fig. 8. A map for evolution of tube conductance D_1, D_2, D_3 in Eq. (5). (a) $P = 1.1$. (b) $P = 2.2$ (c) $P = 3.3$.

with given P are as follows: $D_1(t)$ and $D_2(t)$ do not go to 0 when $\bar{D}_u < D_2(P) < D_1(0)$, only $D_2(t)$ goes to 0 when $D_2(P) < \bar{D}_u < D_1(0)$, and both $D_1(t)$ and $D_2(t)$ goes to 0 when $D_2(P) < D_1(P) < \bar{D}_u$ or no positive fixed points exist. Because of $D_1(0) > D_2(P)$, it is never happened that only $D_1(t)$ goes to 0 and $D_2(t)$ does not goes to 0. Therefore, it means that $D_2(t)$ disappears easier than $D_1(t)$ does, and can be good explanation of asymmetric result of our experimental result as Fig. 5

As shown in Fig. 9, asymptotic behavior of $D_i(t)$ depends on P and D_0. Figure 10 shows some typical examples of transitions as P increases, and it shows what pattern comes next to what depends on a value of D_0. A case shown in Fig. 10a happens when D_0 is much larger than D_s, On the other hand, another case shown in Fig. 10c corresponds to the case when D_0 has very small value, and tubes never grow even in a dark area. Therefore those intial conditions, shown in Figs. 10a and c, are not adequate for our experimental setting.

From the above discussion, D_0 must have an intermediate value, and $D_0 = 0.4$, for example, is one of the appropriate initial condition. It can be seen that using $D_0 = 0.4$ as the initial condition is not only appropriate but also good to mimic our experimental results as shown in Fig.10b. We thus explain our experimental result by using a mathematical model which has nonlinearity of tube developing law. The model showed the saddle-node bifurcation when we changed the illumination period P, which together with a dependency on initial conditions explains the experimental outcome.

4. Discussion

The type of structure created by *Physarum* depends strongly on the frequency of the lighting conditions. Long periods of lighting leads to a separation of the organism, while shorter periods produce

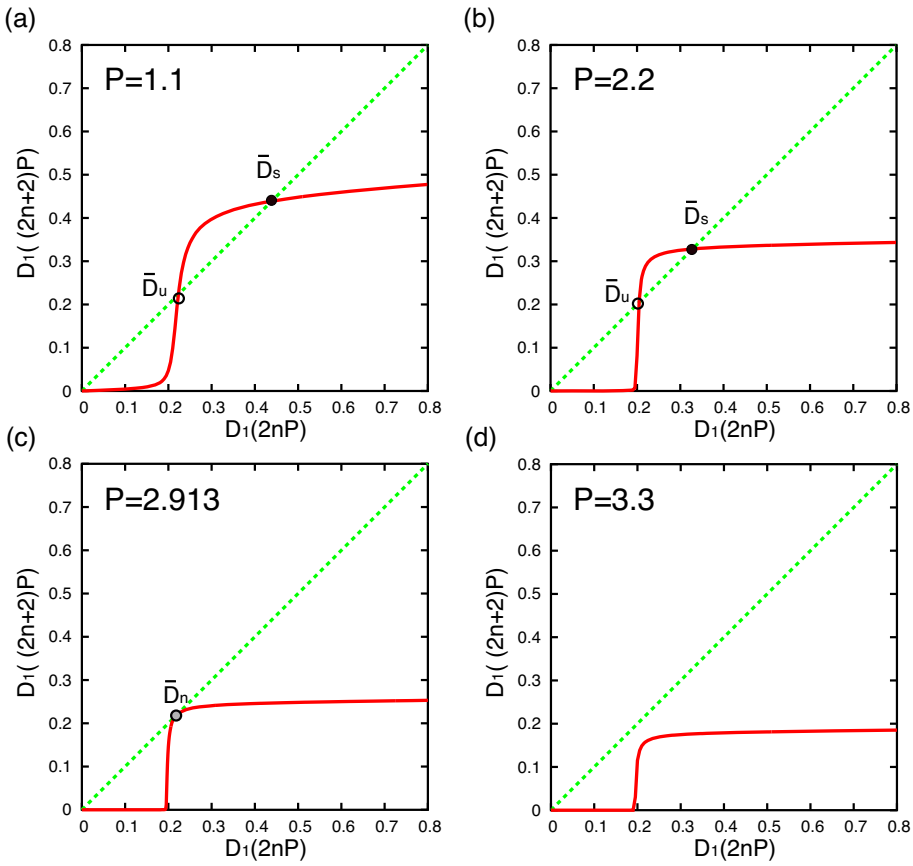

Fig. 9. $D((2n+2)P) = M(D(2nP))$ for several P. All figures are obtained in the numerical calculation. (a) $P = 1.1$, (b) $P = 2.2$, (c) $P = 2.913$ and (d) $P = 3.3$. If we set $D_1(0) = D_2(0) = 0.4$ as same initial conditions in Fig. 8, $D_2(P)$ and magnitude relations are as follows: (a) $D_2(P) = 0.269$, $\bar{D}_u < D_2(P) < D_1(0)$, (b) $D_2(P) = 0.0746$, $D_2(P) < \bar{D}_u < D_1(0)$, (c) $D_2(P) = 0.0188$, $D_2(P) < \bar{D}_n < D_1(0)$, (d) $D_2(P) = 0.00867$, no positive fixed points.

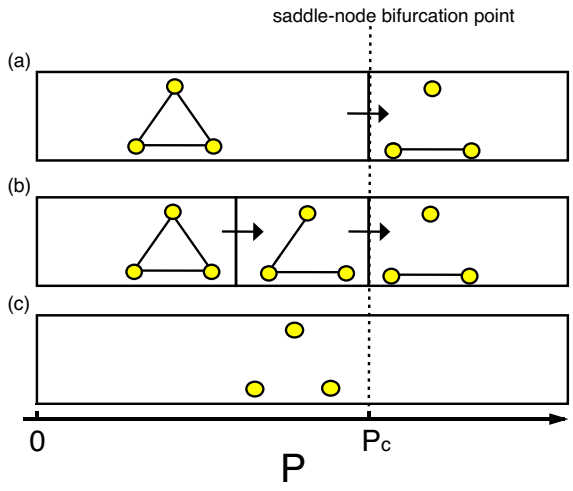

Fig. 10. Schematic illustration of transition of final patterns as P increases. (a) D_0 is very large so that $D_2(2P_c) > \bar{D}_n$. (b) D_0 has an intermediate value including $D_0 = 0.4$. (c) D_0 is lower than any $\bar{D}_u$ and $\bar{D}_n$. D_0 is also lower than $D_u(1.5)$. P_c represents a saddle-node bifurcation point, and $P_c = 2.913$ at $\beta = 0.03$ and $\gamma = 3.0$.

a highly connected structure. For 90 minute period of illumination, the half illuminated tube still spans the illuminated region and the dark region. From a physiological viewpoint, the tube can be used for rapid escape from the illuminated region to the dark region if the condition of either regions gets worse.

For shorter periods of illumination we see a full connection preserved. For $P = 60$ min. a difference can be observed between right side and left side as shown in Fig. 3c. This means final network depends on which side was illuminated first. As tubes were quite thin in initial stage of the experiment, it took relatively short time until they died out in the earlier illuminated region as show in Fig. 5. However, some tubes in the later illuminated region can survive, because these tubes became thick enough in the dark to survive for 60 min. As a consequence, the final connection of all FSs is not likely to collapse. This explanation is supported by our mathematical model. Tubes have to fall below a critical level during a period of illumination in order to be removed.

The changes in structure is evidence of a tradeoff between the need to stay connected in the need to avoid light. Similar tradeoffs have been observed in the migration of *Physarum* to food and away from light [4, 8, 14]. It is notable that the primitive unicellular organism, which has no nervous system, can adjust its foraging structure in response to temporal variations in the environment. The organism manages to select the strategy for risk reduction using only local information. Again, the non-linearity in the model combined with changes in initial conditions are sufficient to explain this tradeoff. It may be said that *Physarum* study is an promising guide way to evolutionary origin of information processing in higher animals.

Acknowledgments

This work was supported by MEXT KAKENHI No. 20300105, Human Frontier Science Program Grant RGP51/2007.

References

[1] T. Nakagaki, H. Yamada, and A. Tóth, "Maze-solving by an amoeboid organism," *Nature*, vol. 407, p. 470, September 2000.

[2] T. Nakagaki, H. Yamada, and A. Tóth, "Path finding by tube morphogenesis in an amoeboid organism," *Biophys. Chem*, vol. 92, pp. 47–52, September 2001.

[3] T. Nakagaki, "Smart behavior of true slime mold in labyrinth," *Res. Microbiol*, vol. 152, pp. 767–770, November 2001.

[4] T. Nakagaki, M. Iima, T. Ueda, Y. Nishiura, T. Saigusa, A. Tero, R. Kobayashi, and K. Showalter, "Minimum-risk path finding by an adaptive amoebal network," *Phys. Rev. Lett*, vol. 99, pp. 068104, August 2007.

[5] T. Nakagaki, H. Yamada, and M. Hara, "Smart network solutions in an amoeboid organism," *Biophys. Chem*, vol. 107, pp. 1–5, January 2004.

[6] A. Tero, S. Takagi, T. Saigusa, K. Ito, D.P. Bebber, M.D. Fricker, K. Yumiki, R. Kobayashi, and T. Nakagaki, "Rules for biologically-inspired adaptive network design," *Science*, vol. 327, pp. 439–442, January 2010.

[7] T. Nakagaki, R. Kobayashi, Y. Nishiura, and T. Ueda, "Obtaining multiple separate food sources: behavioural intelligence in the *Physarum* plasmodium," *Proc. R. Soc. Lond. B*, vol 271, pp. 2305–2310, November 2004.

[8] T. Latty and M. Beekman, "Food quality and the risk of light exposure affect patch-choice decisions in the slime mold *Physarum polycephalum*," *Ecology*, vol. 91, pp. 22–27, January 2010.

[9] T. Latty and M. Beekman, "Food quality affects search strategy in the acellular slime mould, *Physarum polycephalum*," *Behav. Ecol.*, vol. 20, pp. 1160–1167, August 2009.

[10] A. Dussutour, T. Latty, M. Beekman, and S.J. Simpson, "Amoeboid organism solves complex nutritional challenges," *Proc. Natl. Acad. Sci. USA*, vol. 107, pp. 4607–4611, Feburuary 2010.

[11] T. Saigusa, A. Tero, T. Nakagaki, and Y. Kuramoto, "Amoebae anticipate periodic events," *Phys. Rev. Lett*, vol. 100, pp. 018101, January 2008.

[12] N. Kamiya, "Protoplasmic streaming, in protoplasmatologia" eds. L.V. Heilbrunn and F. Weber, vol. 8, pp. 1–199, Springer-Verlag, Vienna, 1959.

[13] D. Kessler, "Plasmodial structure and motility" in *Cell Biology of Physarum and Didymium*, eds. H.C. Aldrich and J.W. Daniel, pp. 145–196, Academic Press, New York, 1982.

[14] T. Nakagaki and R. Guy, "Intelligent behaviors of amoeboid movement based on complex dynamics of soft matter," *Soft Matter*, vol. 4, pp. 57–67, 2008.

[15] T. Nakagaki, A. Tero, R. Kobayashi, I. Onishi, and T. Miyaji, "Computational ability of cells based on cell dynamics and adaptability," *New Generation Computing*, vol. 27, pp. 57–81, January 2009.

[16] A. Tero, R. Kobayashi, and T. Nakagaki, "Mathematical model for adaptive transport network in path finding by true slime mold," *J. Theor. Biol*, vol. 244, pp. 553–564, February 2007.